Thermal, Morphological, and Mechanical Characterization of Novel Carbon Nanofiber-Filled Bismaleimide Composites

M. I. Faraz,[1] S. Bhowmik,[1] C. De Ruijter,[1] F. Laoutid,[2] R. Benedictus,[1] Ph. Dubois,[2] J. V. S. Page,[3] S. Jeson[3]

[1]*Department of Structural Integrity, Faculty of Aerospace Engineering, Delft University of Technology, Delft, The Netherlands*
[2]*Materia Nova asbl, Parc Initialis, Avenue Copernic 1, Mons 7000, Belgium*
[3]*Department of Chemistry and Chemical Engineering, Royal Military college of Canada Kingston, Ontario, Canada*

Received 10 July 2009; accepted 19 November 2009
DOI 10.1002/app.31842
Published online 7 April 2010 in Wiley InterScience (www.interscience.wiley.com).

ABSTRACT: Novel carbon nanofiber (CNF) -filled bismaleimide composites were fabricated by a thermokinetic mixing method. The thermal and mechanical properties of composites containing 1 wt % and 2 wt % CNFs were investigated. Thermogravimetric analysis demonstrated that minimal improvement in thermal stability of the nanocomposites was obtained by the addition of CNFs. Dynamic mechanical analysis showed an increase in storage modulus (E') and glass transition temperature (T_g) upon incorporation of nanofibers. Limiting oxygen index (LOI) has also been found to increase with incorporation of CNFs. Morphological studies of fractured surfaces of the composites has been carried out by scanning electron microscopy to determine the effect of fiber content and dispersion on the failure mechanism. In general, good dispersion was observed, along with agglomeration at some points and some fiber matrix interfacial debonding. A decrease in mechanical strength has been observed and debonding was found as the main failure mechanism. Further research outlook is also presented. © 2010 Wiley Periodicals, Inc. J Appl Polym Sci 117: 2159–2167, 2010

Key words: nanocomposites; thermogravimetric analysis; mixing; fracture; mechanical properties

INTRODUCTION

In recent years, polymer nanocomposites have received more and more attention owing to many competitive advantages like high strength, high stiffness, thermal stability, electrical conductivity, and thermal conductivity. The incorporation of nanoparticles, such as carbon nanotubes and nanoclays, have shown to produce remarkable improvements in mechanical and physical properties of polymers.[1–7] Therefore, at present, the addition of nanoparticles is seen as a potential method for tailoring polymer properties to desired applications. We refer to Refs. [8,9] for more extensive reviews on nanocomposites structure, dispersion issues, properties, and research developments.

The discovery of carbon nanotubes has generated significant attention in the field of material science due to their exceptional mechanical, electrical, and thermal properties in combination with being lightweight. Tensile moduli and strength values, ranging from 270 GPa to 1 TPa and 11–200 GPa, respectively, have been reported for carbon nanotubes.[10,11] This outstanding strength makes it hundred times stronger than steel at one-sixth of the weight, making it desirable to extend its theoretical nanoscale properties to macroscale composite materials.[12] Carbon nanotubes (CNT) are categorized into single-wall (SWNT), multi-wall (MWNT) nanotubes, and carbon nanofiber (CNF) depending upon their diameter. Carbon nanofiber has diameter ranging about 60–200 nm, whereas SWNT and MWNT have 0.7–1.5 nm and 10–50 nm, respectively.[13]

Fiber reinforced composites are widely used in aerospace, civil and military applications due to their high specific strength. It is greatly desired that structural composites must perform well in the harsh multifactor environment. Potential applications of polymer composites in the fields of aerospace, electronic hardware, and automobiles are placing demands for materials with higher thermal stability, higher electrical and thermal conductivity, and improved electromagnetic transparency. Because of the exceptional nanoscale behavior of CNFs in each of these areas, it is plausible that the behavior of polymeric composites could be improved through

Correspondence to: M. I. Faraz (engriftikhar72@yahoo.com).

Contract grant sponsors: Faculty of Aerospace Engineering Delft University of Technology, The Netherlands; Higher Education Commission of Pakistan.

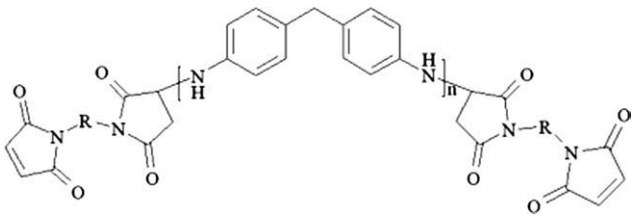

Figure 1 Chemical structure of homide 250.

the addition of CFNs. This was the motivation behind this study.

Carbon nanofibers were selected as filler for the present investigations by virtue of their outstanding performance with respect to the aforementioned challenges. Carbon nanofibers were selected in favor to CNTs because they can be produced industrially at low cost and high production volume.[9] The use of CNFs within thermoplastics has been shown to improve performance by several researchers.[13–17] Ghose et al. have fabricated CNF composites with high-temperature polyimide (PETI 330) for high-performance applications. Thermal and electrical conductivity were improved but voids were found in the samples, so mechanical properties were not improved.[18]

Before starting this study, selection of matrix resin for nanocomposites was of utmost importance. It is reported that polyimides are excellent high-temperature resins for high-performance composites. However, their processability and void formation due to volatiles is still a problem to be addressed. A subclass of polymides known as bismaleimides have a high stability at high temperatures and good hot/wet performance and have attracted attention in the advanced composite industry due to their high performance to cost ratio. It has been demonstrated that bismaleimides show retention of properties at elevated temperature, dimensional stability, low shrinkage, and good mechanical strength, as well as, high resistance against various solvents, acids, and water.[19] Bismaleimides can be processed under epoxy-like conditions, but excel in physical and mechanical properties compared with epoxy. However, because of a high cross-link density, they are very brittle and have low damage tolerance. Much of the research efforts have emphasized primarily on structural modification to improve toughness, processability, and cost.[20–26]

A high-temperature bismaleimide prepolymer, commercially available as "Homide 250," developed by Hos-Technik, having a structure shown in Figure 1 was selected for this study.

The presence of rigid maleimide groups and high cross-link density after curing results in high thermal stability with low volatile emissions. Melting point is merely in the range of 90–120°C which makes processing easier. State of the art literature reveals the availability of bismaleimide and epoxy with nanostructured CNT/CNFs. Corresponding literatures reveal that only few examples are available on bismaleimide and epoxy polymer containing CNT or CNF nanoparticles.[27–29] Therefore, considerable scope remains open for further research to investigate other different areas. In addition, all previous efforts were focussed with two component systems, and solution mixing techniques which are time consuming, at high cost, and having low output. In this study, melt blending technique, which is most common for thermoplastics, is attempted by using a high-speed thermokinetic mixer, specially designed for handling systems which are difficult to disperse. To our knowledge, this is the first study to examine the use of such a high shearing mixer to disperse carbon nanofibers in BMI. Therefore, this article opens a new window for dispersing nanofillers in BMI and other thermoset resins. There exist large research opportunities to answer more fundamental questions regarding dispersion, optimization of filler content, new potential applications, development of processing technologies, filler-matrix interface interactions, and characterization techniques. The objective of this study was to prepare BMI/CNFs composites by a thermokinetic mixing method and examine its thermal and mechanical behavior by using thermogravimetric analysis (TGA) and DMA, respectively. A detailed morphological analysis of fractured surfaces is presented by using scanning electron microscopy (SEM) to investigate failure mechanism, fiber dispersion, and CNF/matrix adhesion.

EXPERIMENTAL

Materials

In this study, a commercially available polymeric resin "Diaminodiphenylmethanebismaleimide-diaminodiphenylmethane copolymer" was purchased from HOS-technik, Austria under the trade name Homide 250. Heat treated, vapor grown carbon nanofibers (PR-19-XT-LHT) having average diameter of 150 nm and length of 50–200 μm were provided by Pyrograf Products, Inc.

Processing of carbon nanofiber bismaleimide nanocomposites

Nanocomposites with 1 and 2 wt % of carbon nanofiber were prepared by melt compounding process. A high thermokinetic mixer "Gelimat blender," (Werner and Pfleiderer Gelimat 1-S) thermokinetic mixer was used to prepare the batches.

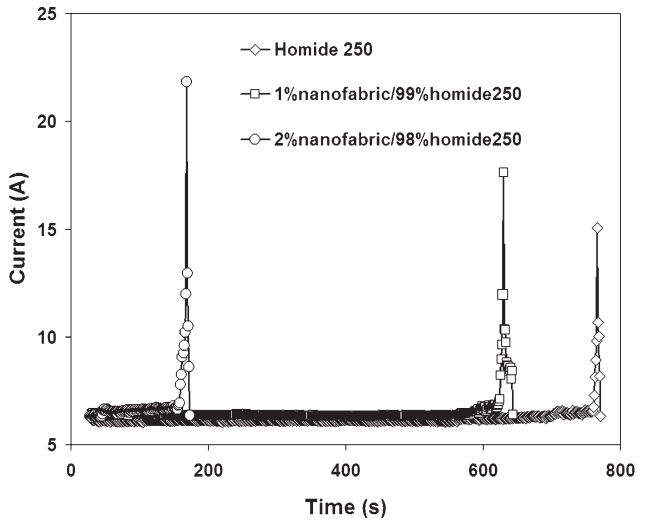

Figure 2 Graph showing increase in energy for nanocomposites processed by Gelimat.

The Gelimat system is specially designed to disperse particles within the polymer by heating, mixing, and compounding, in a period of a few minutes to minimize any thermal degradation of the material. High-speed rotating blades of the Gelimat accelerate the particles and impart high-kinetic energy which is converted to thermal energy upon hitting the chamber walls. Factors like rotor speed, charge size, and material properties dictate compounding time.[30]

The Gelimat was run at a shaft speed of 2000 rpm (13.8 m/s at the tip of the blade) at a temperature of 130°C. This temperature was selected based on rheological results, since at this temperature, the resin is fully melted and has lowest viscosity. At higher temperatures, the gel time of BMI decreases rapidly and it starts curing at 160°C. A quantity of 300 g of material was fed into the thermokinetic mixer for each batch, resulting in an output of 265 g after compounding.

Rectangular specimens (dimensions 110 × 40 × 3 mm) were prepared by compression molding using a 100 Ton Joos press with controlled heating and pressure. The consolidation temperature, pressure, and time were 200°C, 60 bar, and 30 min, respectively. After molding, they were postcured at 220°C for 10 h. Specimens for tensile testing were cut from this molded bar with dimensions according to ISO-527.

Characterization

Thermal analysis

Thermal stability of the polymer and nanocomposites was studied by TGA using a Perkin Elmer Pyris Diamond TG/DTA at a heating rate of 10°C/min under both nitrogen and air atmosphere from 25 to 800°C. Dynamic mechanical analyses were performed by Perkin Elmer Diamond DMTA, using small rectangular specimen with dimensions of 50 × 5 × 3 mm under a nitrogen atmosphere at a heating rate of 10°C/min and a frequency of 1 Hz.

Mechanical testing

Tensile tests of the samples were carried out by using a Zwick 20 KN static tensile test machine (model 1455) at a testing speed of 5 mm/min according to ISO 527-1. Five specimens were tested for each sample and average tensile strengths are reported.

Sample characterization

The morphologies of the fractured tensile specimens and CNFs dispersion in the composite samples were evaluated using SEM model (Jeol JSM-7500F) operated at an accelerated voltage of 40 kV.

Fire testing

Limiting Oxygen Index (LOI), a standard test method to measure the minimum concentration of oxygen for sustaining candle like downward flame combustion, was measured on specimens 80 × 10 × 3 mm according to ISO 4589.

RESULTS AND DISCUSSION

Gelimat mixing

The excellent dispersing properties of the Gelimat thermokinetic mixer can be used to increase the surface area between the polymer and nanoparticles. High shear stresses generated by the equipment have the potential to breakdown aggregates and disperse the reinforcing particles in the polymer matrix.[31] Compounding time as a function of current (ampere) of the neat polymeric resin and nanocomposites is shown in Figure 2. The data obtained by the Gelimat run, i.e., energy required (current), induction time (which is the time difference between the moment the blends are inserted into the mixing chamber and the blends have reached the melting point), consolidation time, and other values are summarized in Table I. The current relates to energy required by Gelimat to melt and mix the polymer

TABLE I
Gelimat-Mixed Homide 250(BMI) Composites Time and Current Values

	Homide 250	1% CNF	2% CNF
Induction time (s)	670	558	130
Peak time (s)	736	600	141
End time (s)	740	604	172
Maximum current (A)	15.0	17.6	21.8

TABLE II
Thermo-Mechanical Properties of Nanocomposites

Sample	$T_{d\ N2}$ (°C)	T_{dair} (°C)	Char (%)	T_g (°C)	Tensile (MPa)	Modulus (GPa)	LOI (%)
0%	380	379	42	235	72	3.8	27.2
1% CNF	387	381	43	245	61	–	28.8
2% CNF	385	381	44	245	58	4.2	29.2

Char taken at 800°C in nitrogen atmosphere. T_d, decomposition temperature; T_g, glass transition temperature obtained from the maximum of the loss modulus; LOI, limiting oxygen index.

with additives. The energy required for the 2% CNF composite is the highest, as indicated in Table I. This can be attributed to an increase in viscosity with increasing nanofiber content. The induction time and mixing time of 2% CNF composite is reduced from 670 s to 130 s and 70 s to 42 s, respectively, when compared with the neat polymer due to the high thermal conductivity of CNFs.

Thermal and flammability properties

To investigate the decomposition behavior of the composites, TGA was performed both in nitrogen and air. The TGA results are summarized in Table II and curves are shown in Figure 3(a,b) for nitrogen and air, respectively. A different behavior is observed depending on the applied atmosphere (air or nitrogen). Under air, the incorporation of

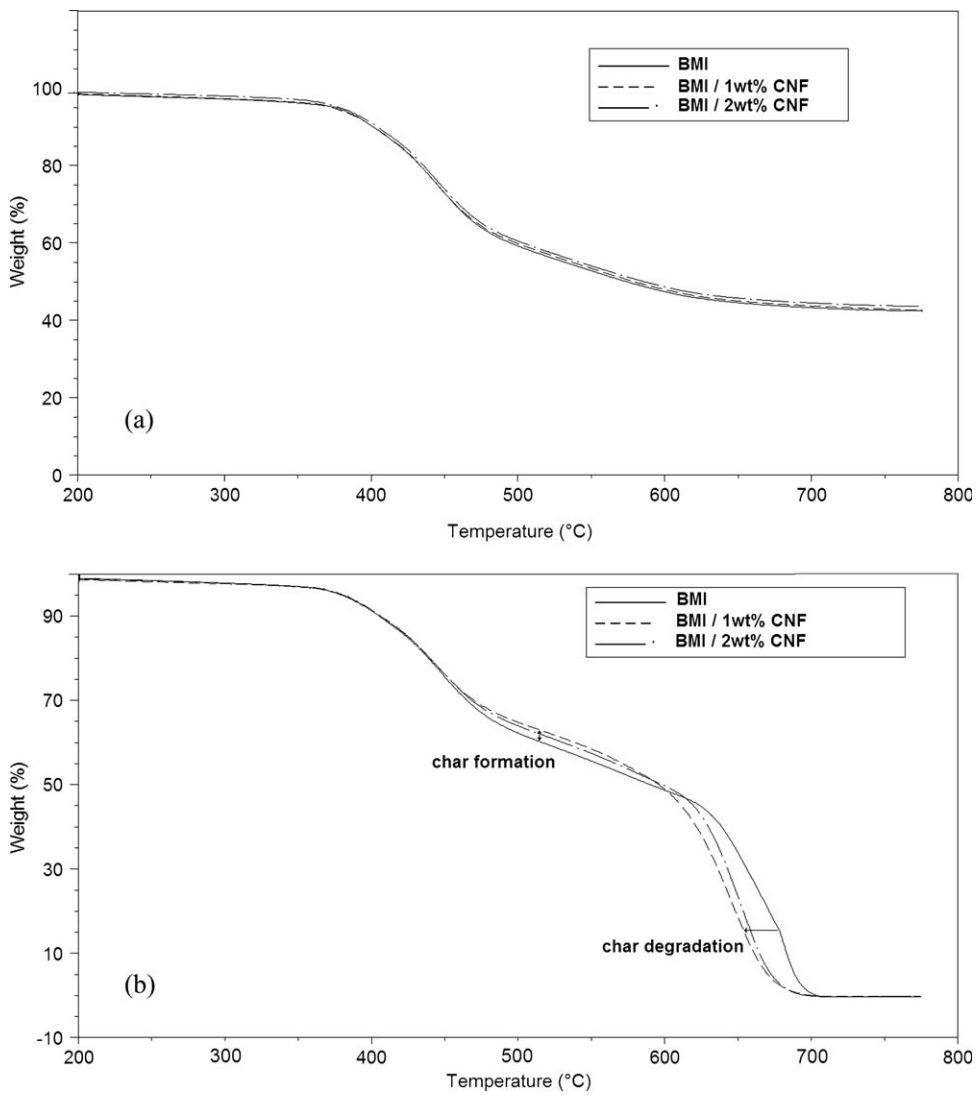

Figure 3 TGA curves showing decomposition behavior run under (a) nitrogen and (b) air.

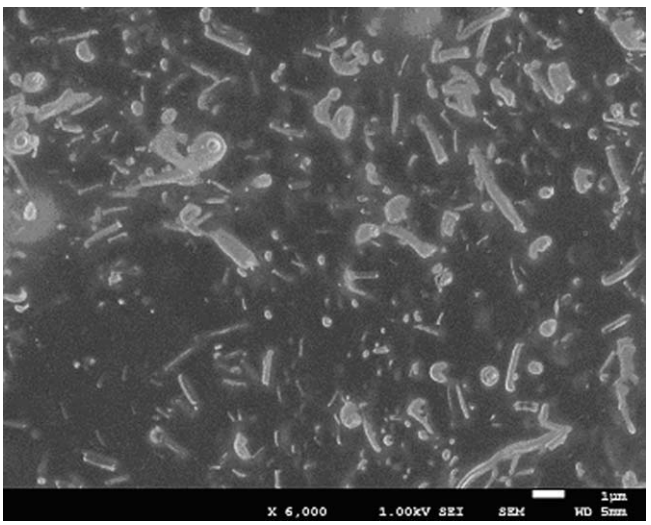

Figure 4 SEM image of a 2% CNF composite after a TGA run in nitrogen showing a network structure of the char left.

CNFs have an effect on the thermal resistance, i.e., the first decomposition step leads to the formation of more char residue. However, this char is less thermally stable in comparison with that formed during thermal degradation of pristine BMI polymer [Fig. 3(a)], it's degradation is accelerated when CNF are used. This is because once the degradation has started, the CNFs played the role of a catalyst to accelerate the decomposition due to presence of iron particulates.[32] It can be seen that the TGA curves are quite stable until the onset of decomposition but after that a very rapid decomposition occurs typically in air [Fig. 3(b)]. The char is thermally stable during nonoxidative thermal decomposition [Fig. 3(a)]. No char is left in air and around 40% char is left in a nitrogen environment. It can be concluded that incorporation of CNFs does not significantly enhance the thermal stability of the corresponding nanocomposite system for the range of fiber concentrations investigated in this study. However, thermal stability is still reasonably high to be acceptable for many advanced technologies. Kashiwagi et al.[33] and Zhou et al.[34] have also observed that thermal stability remains insensitive to the incorporation of CNFs. It can be affected by physiochemical bonding states and microstructural features of the composites, including attendant branching and stiffening effects,[35] which needs to be investigated further.

Limiting Oxygen Index (LOI) is a very common method to assess flammability of polymers. A high value of this index is a sign of low flammability and less easily ignited materials. The addition of CNF has increased the LOI value from 27.2 to 29.2 as shown in Table II. This indicates that CNFs also act as flame retardant. The decreased flammability can be attributed to the formation of cohesive char residue.[32,36] The char left after the TGA run in nitrogen showed a very integrated morphology, free of any cracks, openings and bubbles as is observed by SEM, shown in Figure 4. Moreover, no dripping was observed during burning, reducing fire spread hazard. This char acts as a barrier to prevent the diffusion of heat and gasses from the flame through the polymer and stops the fuel, i.e., degraded products, to reach the flame.[33,36] However, when CNFs only are added to a resin, the effect on flame retardancy will not be sufficient to pass the regulatory standards, but in combination with a suitable flame retardant a synergistic effect might be expected.[37] In the near future, endeavors will be made in this direction as well.

Dynamic mechanical analysis has been performed to determine the dynamic mechanical properties and viscoelastic behavior. An increase in glass transition temperature (T_g) of about 10°C was observed for the nanocomposites as given in Table II. Glass transition temperatures were determined from the maximum of the loss modulus (E'') curves as shown in Figure 5(b). This increase in T_g could be attributed to

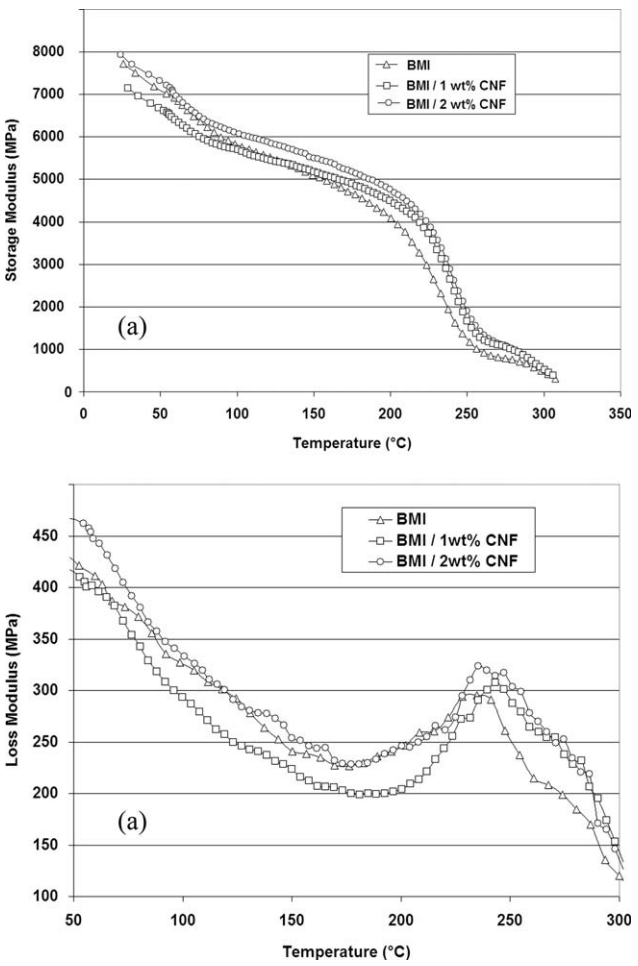

Figure 5 DMA curves of nanocomposites (a) storage modulus (E') (b) Loss modulus (E'').

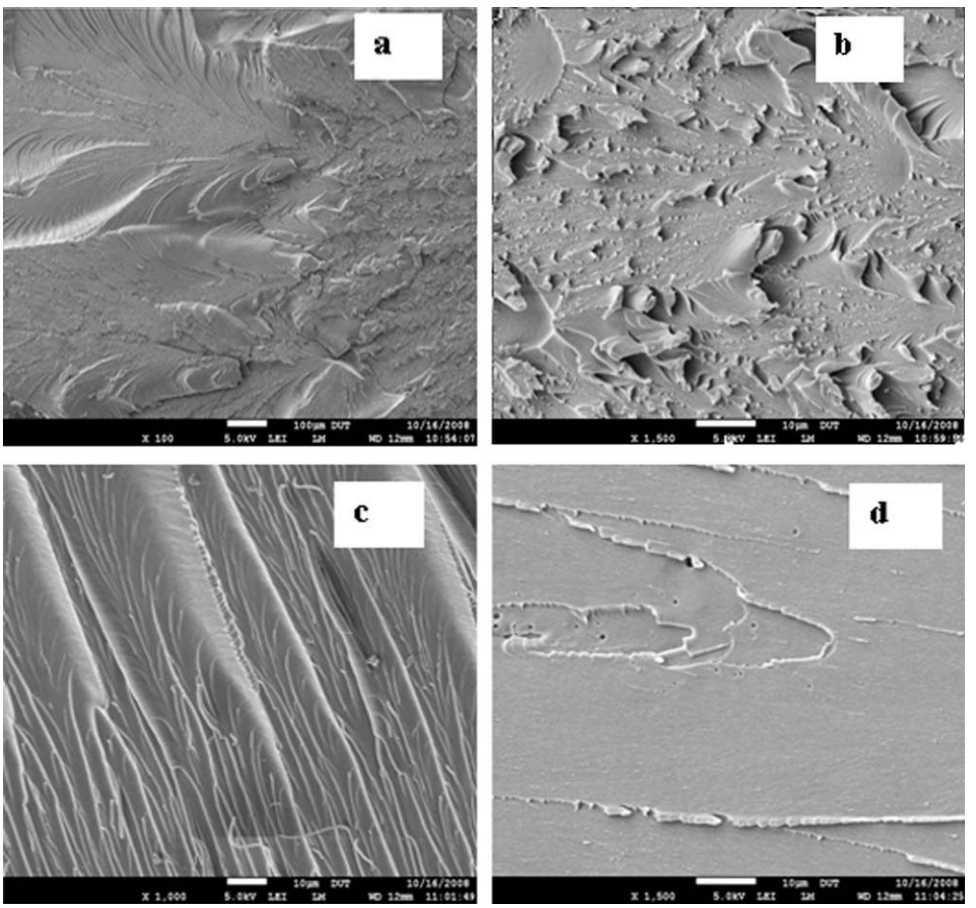

Figure 6 SEM images of fractured surface of neat BMI at different locations and magnifications. (a) fracture initiation; (b) matrix tearing; (c) cleavage planes; (d) brittle failure.

constrained chain mobility imposed by rigid CNFs.[34,38] This conclusion is further supported by increase in storage modulus E' of the nanocomposites compared with the neat polymer as shown in Figure 5(a). The improvement of the storage modulus is more significant above T_g. The storage modulus increased from 1238 MPa to 1900 MPa at 250°C for 2% of CNFs, i.e., an improvement of 53%. The rigid CNF network structure formed is playing a key role for this phenomenon.[39]

Mechanical properties

The mechanical properties of the composites depend on many factors, including filler aspect ratio, degree of dispersion, filler-matrix adhesion, residual thermal stresses which may cause filler-matrix debonding, and the presence of voids. The average tensile strength values for BMI/CNFs composites are reported in Table II. Five specimens were tested for each formulation. All specimens failed in a brittle manner, and no obvious yield point was found in the tensile curves, which are not shown here for brevity purpose. A decrease in tensile strength is observed for each composition in comparison to the neat polymer and tensile strength is decreasing with increasing fiber content. There was some fiber bundles observed with 2 wt % of CNF as shown in Figure 7(e) by SEM fracture analysis. These fiber bundles may act as stress concentration sites upon loading and result in premature failure. The findings of present investigation is in line with many other researchers, who have also observed that higher concentration of CNFs did not perform well, in terms of mechanical properties which could be due to the formation of voids and other defects[27,39,40] and as a consequence results in reduction of the tensile strength. It is also obvious that there is more resistance to deformation in the presence of CNF as can be seen from Figure 7(a,d). This reduced deformation of nanocomposites is due to the formation of strong crosslinking network of CNF with matrix which results in restriction of polymer chain mobility of amorphous phase and hence the reduced flexibility.[39,40] This increase in stiffness is also confirmed by the increase in elastic modulus of the nanocomposites as shown in Table II. Hence, carbon nanofibers have reinforcing effect both below and above glass transition temperature. Fiber pull-out effect is dominant for each formulation as shown in Figure

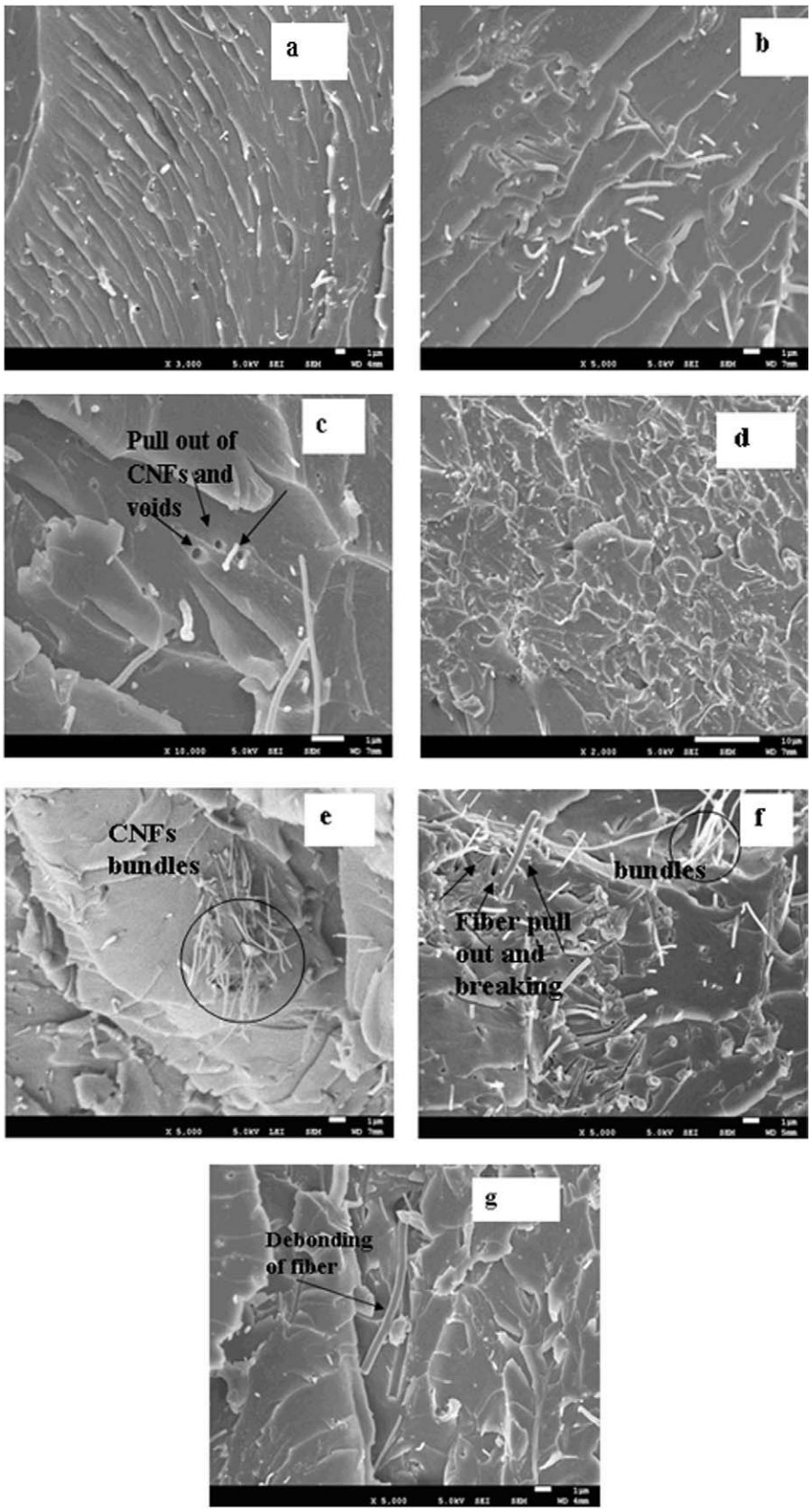

Figure 7 SEM images of fractured surfaces of BMI/CNFs nanocomposites containing 1 wt % (a–c) and 2 wt % (d–g) of CNFs, at different locations and magnifications.

7(c,f,g). The absence of matrix material on the nanofibers together with the presence of voids indicates complete pull-out and concludes there is weak adhesion between the nanofibers and the matrix. The lower interfacial adhesion results in inefficient load transfer between the fiber and matrix and failure will occur at lower loading.[41] This behavior has also been observed by other researchers and they have shown that chemical functionalization could be an effective solution to improve the dispersion and adhesion for enhancing stress transfer.[27,39] The behavior of the present system after chemical treatment of the nanofibers will be future scope of research. Thermal stresses induced during curing of thermosets, due to mismatch of the thermal expansion coefficients of the components will be detrimental to the mechanical strength. Also, crystallization and shrinkage may negatively affect the composite properties. This is also an interesting area to be explored further to improve the present system.

Morphological study of BMI/CNFs composites

SEM was used to observe the surface morphology and nanofiber dispersion of tensile fractured surfaces. All the images were taken from crack propagation areas, at different magnifications.

Figure 6(a–d) shows SEM images of neat BMI fractured surfaces. The surface close to the initial crack is relatively smooth. Obvious cleavage steps and cleavage plains are observed as shown in Figure 6(a). Further away from the initial crack, the surface appears rougher and matrix tearing takes place [Fig. 6(b)] which could be observed at a higher magnification. A number of small cleavage planes are observed in rougher surfaces as shown in Figure 6(c). A smooth and flat surface is observed at higher magnification between the cleavage steps [Fig. 6(d)] which is showing a typical brittle failure.

In Figure 7(a–g), fractured surfaces of nanocomposites with 1 wt % (a–c) and 2 wt % (d–g) of CNFs are shown. The nanocomposites surfaces [Fig. 7(a,d)] are rougher when compared with the neat matrix. It shows that carbon nanofibers are distorting the crack propagation and more energy is dissipated in fracture. Overall, there is a uniform distribution of CNFs within the polymer matrix at 1 wt % as shown in Figure 7(a,b). However, the nanofibers are broken or pulled out of the matrix and there is no matrix material observed around the fibers as shown in Figure 7(b,c). This indicates a poor adhesion between the fibers and the matrix. It is also exhibited that at some points, the nanofibers are completely pulled out, and voids are formed as shown by arrows in Figure 7(c). These voids consume more energy for fracture, and therefore, a more rough surface is observed, although it fails at lower load.[27]

At a concentration of 2 wt % of CNFs, at some points bundles are formed, as shown in Figure 7(e,f) pointed by circles. These bundles act as stress concentration points and result in prefracture failure.[27,39] There is increase in fiber pull-out and debonding at higher loading as shown in Figure 7(f). A more zoomed view of a debonded fiber is shown in Figure 7(g) pointed by an arrow. Therefore, it can be concluded that deboning is the dominant failure mechanism in this investigation.

CONCLUSIONS

A new BMI prepolymer was reinforced successfully with CNF (1 and 2 wt %) by using an innovative melt compounding technique, i.e., high shear thermokinetic mixer. The method used is very first experience with the BMI nanocomposites saving much time and having high output. The reinforcing of CNF caused restriction of polymer chain mobility which was confirmed by the increase of the storage modulus and the glass transition temperature as measured by DMA.

The incorporation of CNFs induces the formation of more char residue in an air atmosphere. However, this char is thermally unstable and degrades faster in comparison with that formed during the thermal decomposition of pristine polymer. Despite the fact that the char formed when CNFs are used degrades at lower temperature, but it protects the polymer during LOI testing.

The poor interfacial adhesion between the CNFs and BMI resin overall along with fiber bundles for high concentration resulted in lower mechanical strength of the nanocomposites due to inefficient load transfer. Uniform dispersion and strong interface adhesion is necessary to get full potential of the nanocomposites. Chemical functionalization can be an effective tool to improve adhesion and to obtain uniform dispersion and will be interest for future investigation.

The authors like to specially thank Prof. V. T. Bui and Prof. H. W. Bonin, Royal Military College of Canada for the use of thermo kinetic mixer in this research. The authors also like to thank Dr. F. Loutid, Materia Nova lab, Mons Belgium for using flammability testing apparatus and helping in result analysis.

References

1. Ray, S. S.; Okamoto, M. Prog Polym Sci 2003, 28, 1539.
2. Wanger, H. D. Nat Nanotechnol 2007, 2, 742.
3. Tai, N.-H.; Yeh, M.-K.; Liu, J.-H. Carbon 2004, 42, 2774.
4. Hammel, E.; Tang, X.; Trampert, M.; Schmitt, T.; Mauthner, K.; Eder, A.; Potschke, P. Carbon 2004, 42, 1153.
5. Njuguna, J.; Pielichowski, K.; Desai, S. Polym Adv Technol 2008, 19, 947.

6. Hackman, I.; Hollaway, L. Proceedings of the International Symposium on Bond Behaviour of FRP in Structures; UK; International Institute for FRP in Construction (IIFC), Hong Kong, China, 2005.
7. Aravind, D.; Szu-Hui, L.; Zhong-Zhen, Y.; Mai, Y.-W. Aus J Chem 2007, 60, 496.
8. Tjong, S. C. Mater Sci Eng R 2006, 53, 73.
9. Thostenson, E. T.; Li, C.; Chou, T.-W. Comput Sci Technol 2005, 65, 491.
10. Li, F.; Cheng, H. M.; Bai, S.; Su, G. Appl Phys Lett 2000, 77, 3161.
11. Lu, J. P. J Phys Chem Solids 1997, 58, 1649.
12. Lau, K.-T.; Hui, D. Compos B 2002, 33, 263.
13. Zeng, J.; Saltysiak, B.; Johnson, W. S.; Schiraldi, D. A.; Kumar, S. Compos B 2004, 35, 173.
14. Coopera, C. A.; Ravicha, D.; Lipsb, D.; Mayerb, J.; Wagnera, H. D. Comput Sci Technol 2002, 62, 1105.
15. Carneiro, S.; Covas, J. A.; Bernardo, C. A.; Caldeira, G.; Van Hattum, F. W. J.; Ting, J.-M.; Alig, R. L.; Lake', M. L. Comput Sci Technol 1998, 58, 401.
16. Kuriger, R. J.; Alam, M. K.; Anderson, D. P.; Jacobsen, R. L. Compos A 2002, 33, 53.
17. Sui, G.; Zhong, W. H.; Ren, X.; Wang, X. Q.; Yang, X. P. Mater Chem Phys 2009, 115, 404.
18. Ghose, S.; Watson, K. A.; Working, D. C.; Siochi, E. J.; Connell, J. W.; Criss, J. M. High Perform Polym 2006, 18, 527.
19. Hamerton, I. High Perform Polym 1996, 8, 83.
20. Stenzenberger, H. D. Comput Struct 1993, 24, 219.
21. Cai, Y.; Liu, P.; Hu, X.; Wang, D.; Xu, D. Polymer 2000, 41, 5653.
22. Hsiao, S.-H.; Chang, C.-F. J Polym Res 1996, 3, 31.
23. Liu, Y.-L.; Chen, Y.-J. Polymer 2004, 45, 1797.
24. Dinakaran, K.; Alagar, M.; Kumar, R. S. Eur Polym J 2003, 39, 2225.
25. Nair, C. P. R. Prog Polym Sci 2004, 29, 401.
26. Gu, A.; Liang, G.; Lan, L. J Appl Polym Sci 1996, 62, 799.
27. Prolongo, S. G.; Campo, M.; Gude, M. R.; Chaos-Morán, R.; Ureña, A. Comput Sci Technol 2009, 69, 349.
28. Liu, L.; Gu, A.; Fang, Z.; Tong, L.; Xu, Z. Compos A 2007, 38, 1957.
29. Aijuan, G.; Liang, G.; Liang, D.; Ni, M. Polym Adv Technol 2007, 18, 835.
30. Gopakumar, T. G.; Page, D. J. Y. S. J Appl Polym Sci 2005, 96, 1557.
31. Gopakumar, T. G.; Page, D. J. Y. S. Polym Eng Sci 2004, 44, 1162.
32. Takashi, K.; Erik, G.; Jenny, H.; Richard, H.; Award, W.; Douglas, J. Macromol Rapid Commun 2002, 23, 761.
33. Takashi, K.; Minfang, M.; Karen, W.; Bani, C.; Raghavan, S. R.; Seongchan, P.; Miriam, R.; Yin, Y.; Eric, G.; John, S.; Richard, H.; Douglas, J. Polymer 2008, 49, 4358.
34. Zhou, Y.; Pervin, F.; Jeelani, S. J Mater Sci 2007, 42, 7544.
35. Seo, M.-K.; Park, S.-J. Mater Sci Eng A 2009, 508, 28.
36. Kashiwagi, T.; Fangming, D.; Winey, K. I.; Groth, K. M.; Shields, J. R.; Bellayer, S. P.; Kim, H.; Douglas, J. F. Polymer 2005, 46, 471.
37. Ye, L.; Wu, Q.; Qu, B. Polym Degrad Stab 2009, 94, 751.
38. Fisher, F. T.; Eitan, A.; Andrews, R.; Schadler, L. S.; Brinson, L. C. Adv Compos Lett 2004, 13, 105.
39. Kumara, S.; Rath, T.; Mahaling, R. N.; Reddya, C. S.; Dasa, C. K.; Pandey, K. N.; Srivastava, R. B.; Yadaw, S. B. Mater Sci Eng B 2007, 141, 61.
40. Lozano, K.; Barrera, E. V. J Appl Polym Sci 2001, 79, 125.
41. Schadler, L. S.; Giannaris, S. C.; Ajayana, P. M. Appl Phys Lett 1998, 73, 3842.